Data-Driven Event Location Identification Without Knowing Network Parameters Using Synchronized Electric-Field and Current Waveform Data

Milad Izadi, *Student Member, IEEE*, Mirrasoul J. Mousavi, *Senior Member, IEEE*, Jong Min Lim, *Senior Member, IEEE*, and Hamed Mohsenian-Rad, *Fellow, IEEE*

***Abstract*—Event location identification is a challenging task in power distribution feeders due to limited number of measurement devices. Another challenge is the lack of access to reliable information on network parameters. This paper proposes a new method to address *both* challenges. We identify the location of the events in distribution feeders using *synchro-waveform measurements* from a group of line-mounted sensors, which are inexpensive and easy to install. Importantly, we do *not* require any prior knowledge about the network parameters, i.e., the impedance of the distribution lines and the loading at each bus. The sensors in this study measure the time-domain waveforms for *electric field* and *current*; they do *not* measure voltage. First, the voltage waveform is approximated from the available electric field waveform measurement. Next, the network parameters are estimated by a novel event-based method using data from a few locationally scarce synchro-waveform measurements. Finally, the location of the event is identified by analyzing a data-driven reconstructed circuit model. The method is applied to *real-world* measurements from a distribution feeder in the United States. Despite not using any knowledge about the network parameters and also using measurements from only a few sensors, the results demonstrate the accuracy and consistency of the proposed framework in identifying the location of the events.**

***Keywords*: Synchro-waveform, electric field waveform measurements, line-mounded sensors, event location identification, model-free method, power distribution feeder, line parameter estimation.**

I. Introduction

In this real-world study, we are provided with the time-synchronized *electric field (e-field) waveform* and *current waveform* measurements from line-mounted sensors [1] at four sites of a three-phase power distribution feeder in the United States[1]. Each sensor can report 130 recordings per cycle, i.e., one sample every 120 μsec [1]. The locations of the sensors are known from their latitude and longitude coordinates. Sensor 1 is at the upstream of Sensor 2, Sensor 2 is at the upstream of Sensor 3, and Sensor 3 is at the upstream of Sensor 4.

Fig. 1 shows an example of the synchronized e-field waveform and current waveform measurements that are captured by the sensors during an *event* on the feeder. Based on visual inspection, we can argue that the event has occurred somewhere on Phase B between Sensor 2 and Sensor 3. The reason for this argument is that, the event causes very large changes in Phase B of the current waveform of Sensor 2, yet it causes very small changes in Phase B of the current waveform of Sensor 3. The question that we seek to answer in this paper is: *can we use only these synchronized e-field and current waveform measurements, without any prior information about the network parameters, and automatically identify the precise location of the event?* We will show that the answer to this question is 'Yes'.

Different methods have been previously proposed to identify the location of events in power systems, including impedance-based methods [2]–[5], traveling wave-based methods [6], and wide area-based methods [7], [8]. Of particular interest here is the work in [8], which uses synchronized waveform measurements from waveform measurement units (WMUs) [7]–[12]. The method in [8] is able to identify the correct location of events in power distribution networks, including transient events, such as incipient faults, and permanent events, such as permanent faults and capacitor bank switching.

The method in [8] requires prior knowledge about the network parameters, namely the impedance of the line segments and the loading of the buses. However, such network information is *not* always available. Also, the method in [8] requires access to the synchronized voltage waveform measurements. However, in practice, the line-mounted sensors *cannot* measure voltage waveforms, instead they measure e-field waveforms.

Since the voltage waveforms and the network parameters are *not* available in this real-world problem, we propose to instead use synchronized e-field and current waveform measurements to identify the location of events in power distribution systems.

The method in this paper is purely data-driven, i.e., it is model-free. It does *not* require any prior information about the network. Hence, this method is very suitable for real-world field implementation, as it is evident from the results that we present in this paper based on real-world field measurements.

II. Voltage Waveform Approximation Based on Electric Field Waveform Measurements

As mentioned earlier, the line-mounted sensors in this real-world analysis do *not* measure voltage; instead, they measure e-field. The e-field and current waveform measurements are provided in *time-domain* whenever an event occurs.

Let $e(t)$ denote the e-field waveform around a line conductor that is measured by a line-mounted sensor; and let $v(t)$ denote the voltage waveform of the conductor. Since line-mounted sensors are installed very close to the conductor, they provide a very good approximation of the shape of the voltage waveform. In particular, e-field waveform measurements are almost in-phase with the voltage waveform of the conductor. Therefore, we can assume the following relationship between the voltage waveform and the e-field waveform at the conductor:

$$v(t) = \beta \times e(t), \qquad (1)$$

where $\beta \geq 0$ is the tuning operator. We can analytically obtain β based on different environmental factors, such as the distance between the conductor and the sensor, the geometry of the conductor, and the dielectric permittivity of free space [13].

M. Izadi and H. Mohsenian-Rad are with the Department of Electrical and Computer Engineering, University of California, Riverside, CA, USA; e-mails: {mizadi, hamed}@ece.ucr.edu. M. J. Mousavi and J. M. Lim are with Sentient Energy, Inc., Santa Clara, CA, USA; e-mails: {mmousavi, jmlim}@sentient-energy.com. The corresponding author is H. Mohsenian-Rad.

[1]We thank Jenya Okuneva for her help in obtaining the real-world data.

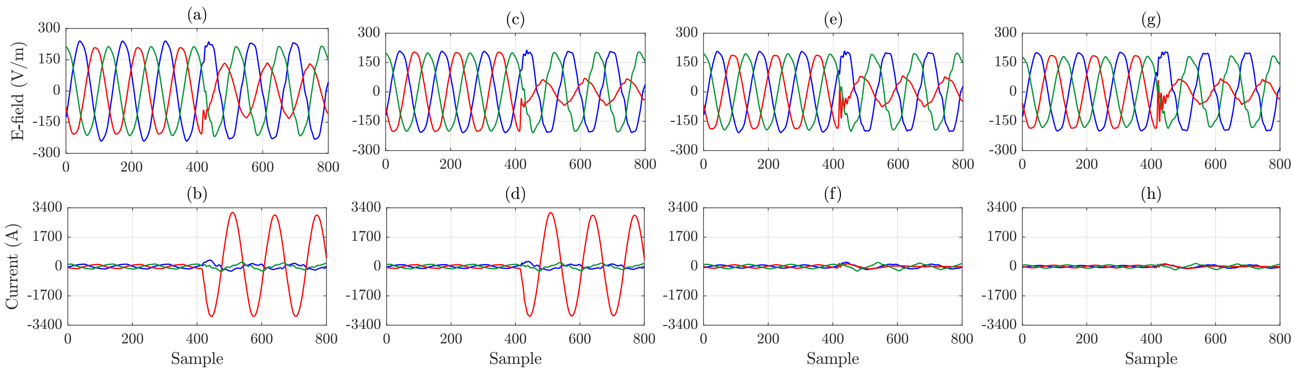

Fig. 1. Real-world synchronized three-phase e-field waveform and three-phase current waveform measurements captured by line-mounted sensors at four sites on a distribution feeder in the United States during an event that occurred on April 26, 2021: (a)-(b) Sensor 1; (c)-(d) Sensor 2; (e)-(f) Sensor 3; (g)-(h) Sensor 4.

However, in this paper, we do *not* need the true value of β, see *Lemma* 1 in Section IV. Instead, we can consider the fact that, under normal grid operating conditions, i.e., in the absence of an event, the voltage at any point on a conductor is very close to the voltage at the substation, where the voltage is measured directly as part of the typical substation monitoring system. Hence, we can assume that the magnitude of voltage waveform during normal operating conditions is available from the voltage measurements at the substation. Thus, we can obtain β in a data-driven fashion based on the peak amplitude of the e-field waveform and the peak amplitude of the voltage waveform during normal conditions and right *before* an event occurs.

For example, again consider the real-world e-field waveform measurements in Fig. 1(a). We can see that, the peak amplitude of the e-field waveform measurements on Phase B of Sensor 1 during the normal operating conditions, i.e., before the event occurs, is about 210 V/m. On the other hand, the under-study feeder is operated at 22.9 kV line-to-line. Thus, the peak amplitude of the voltage waveform during normal conditions is obtained as $22.9 \times 1000 \times \sqrt{2}/\sqrt{3} = 18,698$ V. Accordingly, we can obtain the tuning operator as $\beta = 18,698/210 = 89$.

Once the tuning operator is obtained, the voltage waveform can be approximated via (1). Therefore, for the rest of this paper, we assume that we have access to the current waveform measurements and the *approximated* voltage waveform measurements at each of the line-mounted sensors.

III. Reconstructing the Unknown Network Parameters

As mentioned in Section I, one key advantage of the proposed method is that we do *not* need any prior knowledge about the network parameters, namely the resistance and inductance of the distribution lines and the loading of the buses. We rather estimate those parameters based on the same measurements that we receive from the existing line-mounted sensors.

A. Intuition

Consider a power distribution feeder that is observed by two line sensors, as shown in Fig. 2(a). Let $i_1(t)$ denote the current waveform measurements and $v_1(t)$ denote the approximated voltage waveform measurements at Sensor 1. Also, let $i_2(t)$ denote the current waveform measurements and $v_2(t)$ denote the approximated voltage waveform measurements at Sensor 2. Suppose an event occurs at time $t = \tau$ at an *unknown* location. For the sake of our explanation, we assume that the event has occurred somewhere at the downstream of the two sensors, i.e., in the area that is marked in the downstream network.

To explain the intuition in obtaining the network parameters, let us first analyze the distribution feeder at one cycle, *right before* the event occurs, i.e., from time $\tau - T$ to time τ, where τ is the time that the event has occurred and $T = 16.667$ msec is the duration of one cycle. Fig. 2(a) shows the distribution feeder for the period from $\tau - T$ to τ. During this period, the feeder is under normal conditions, i.e., there is no event. Once the event occurs at $t = \tau$, the event current is injected to the network, as shown in Fig. 2(b). Given the waveforms *right before* the event occurs, i.e., from $\tau - T$ to τ, and the waveforms *right after* the event occurs, i.e., from τ to $\tau + T$, we can obtain the amount of changes in voltage waveforms and current waveforms at Sensors 1 and 2 as follows:

$$\begin{aligned}
\Delta v_1(t) &= v_1(t) - v_1(t-T), && t = \tau, \cdots, \tau + T, \\
\Delta v_2(t) &= v_2(t) - v_2(t-T), && t = \tau, \cdots, \tau + T, \\
\Delta i_1(t) &= i_1(t) - i_1(t-T), && t = \tau, \cdots, \tau + T, \\
\Delta i_2(t) &= i_2(t) - i_2(t-T), && t = \tau, \cdots, \tau + T.
\end{aligned} \tag{2}$$

By comparing the feeder *right before* the event occurs, as in Fig. 2(a), and the feeder *right after* the event occurs, as in Fig. 2(b), it is expected that the network parameters, including the line parameters and load parameters, remain the same. The reason comes from the fact that, once the event occurs, most of the event current is injected into the upstream network, because the Thevenin impedance of the upstream network is much smaller than the impedance of the load points [12]. In other words, almost all of the event current flows from the event location to the upstream network, as shown with the red line in Fig. 2(c). Accordingly, the currents of the lines between Sensor 1 and Sensor 2 are the same. Thus, the changes in current waveforms at Sensor 1 and Sensor 2 are almost the same:

$$\Delta i_1(t) \simeq \Delta i_2(t), \qquad t = \tau, \cdots, \tau + T. \tag{3}$$

Thus, we can simplify the feeder between Sensor 1 and Sensor 2 during the event. That is, we can assume that there is no load points between the two sensors during the event, see Fig. 2(c). It should be noted that, the intuition is less reliable when the event causes very small changes in the waveform measurements.

B. Using Regression to Estimate Line Parameters

From Section III-A, we can focus our analysis during the event on the simplified distribution feeder model in Fig. 2(c). In this simplified model, the nodal voltages are the *changes* in the voltage waveforms between the two successive cycles, one cycle right after the event and one cycle right before the event, as in (2). Similarly, the line currents are the *changes* in current waveforms between the two successive cycles, one cycle right

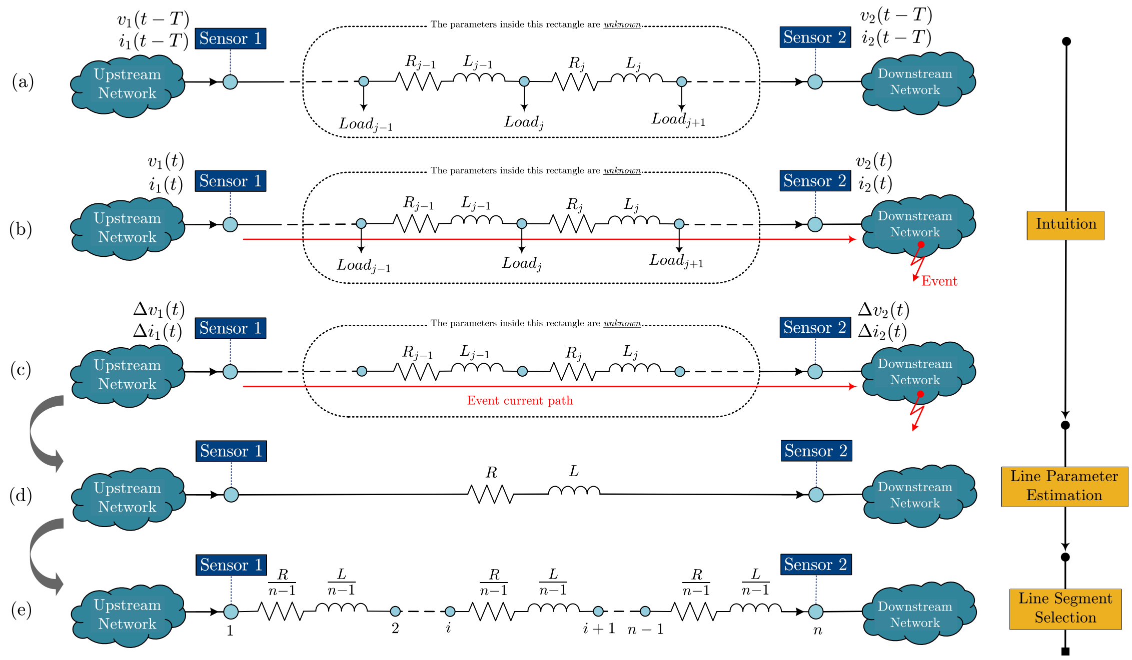

Fig. 2. An illustration to reconstruct an unknown distribution feeder between two sensors to a known distribution feeder: (a) the feeder at one cycle *right before* the event; (b) the feeder at one cycle *right after* the event; (c) the difference between right after the event and right before the event; (d) the combined line parameters; (e) the reconstructed feeder model with even line parameters. The parameters inside the rectangle in (a)-(c) are unknown.

after the event and one cycle right before the event, as in (2). As a result, the line parameters of the line segments between Sensor 1 and Sensor 2 are connected in *series*, see Fig. 2(c).

Let R_j and L_j denote the resistance and the inductance of line segment j, respectively. Considering the series connection of the line parameters between Sensor 1 and Sensor 2 in Fig. 2(c), at each time $t = \tau, \ldots, \tau + T$, we can write the voltage difference in time-domain between the two sensors as:

$$\begin{aligned}\Delta v_1(t) - \Delta v_2(t) &= \sum_{j\in\mathcal{S}} R_j \Delta i_1(t) + \sum_{j\in\mathcal{S}} L_j \frac{d\Delta i_1(t)}{dt}, \\ &= R\Delta i_1(t) + L\frac{d\Delta i_1(t)}{dt},\end{aligned} \tag{4}$$

where $\mathcal{S}$ is the set of all the line segments between Sensor 1 and Sensor 2; R is the combined resistance that is obtained by adding up all the line resistances between Sensors 1 and 2; and L is the combined inductance that is obtained by adding up all the line inductances between Sensors 1 and 2. Fig. 2(d) shows the distribution feeder model with the combined line parameters R and L. We can write (4) in matrix form as:

$$\Delta V = \Delta I \; P, \tag{5}$$

where

$$\Delta V = \begin{bmatrix} \Delta v_1(\tau) - \Delta v_2(\tau) \\ \Delta v_1(\tau + \Delta t) - \Delta v_2(\tau + \Delta t) \\ \vdots \\ \Delta v_1(\tau + T) - \Delta v_2(\tau + T) \end{bmatrix}, \tag{6}$$

$$\Delta I = \begin{bmatrix} \Delta i_1(\tau) & \frac{d\Delta i_1(\tau)}{dt} \\ \Delta i_1(\tau + \Delta t) & \frac{d\Delta i_1(\tau+\Delta t)}{dt} \\ \vdots & \vdots \\ \Delta i_1(\tau + T) & \frac{d\Delta i_1(\tau+T)}{dt} \end{bmatrix}, \quad P = \begin{bmatrix} R \\ L \end{bmatrix}, \tag{7}$$

where $\Delta t = 120$ μsec is the sensors' reporting interval [1].

We can estimate the line parameters in (5) by using the regression method with the following closed-form solution:

$$\hat{P} = (\Delta I^T \Delta I)^{-1} \Delta I^T \Delta V, \tag{8}$$

where $\hat{P}$ is the estimation of the unknown line parameters.

C. Selecting the Number of Line Segments

Utility poles are used to carry overhead lines. For the sake of our analysis, we treat each pole as a bus for the feeder. Even in the absence of the utility model, the location of the utility poles can be detected by using aerial images, Google street view images, or field surveys [14]. Even if the location of the poles is not known, we can use the fact the distance between every two adjacent utility poles are usually equal. Thus, another option to obtain the number of poles is to use the distance between two sensors and the typical distance between two adjacent poles. It bears mentioning that, in cable networks, we treat each pad mounted box as a bus for the feeder.

Suppose the distance between two sensors is D and the distance between two adjacent poles is h. The number of poles between the two sensors is approximately obtained as:

$$n = [D/h] + 1, \tag{9}$$

where $[\cdot]$ returns the integer part. For example, the distance between Sensor 1 and Sensor 2 in Fig. 2 is 12670 ft and the typical distance between two adjacent poles of the under-study feeder is 150 ft. Thus, the number of poles/buses between Sensor 1 and Sensor 2 is $n = 85 = [12670/150] + 1$.

We number the buses from bus 1, where Sensor 1 is installed, to bus n, where Sensor 2 is installed, see Fig. 2(e). The number of line segments between the two sensors is $n - 1$. From (8), we obtain the resistance of each line as $R/(n-1)$ and the inductance of each line as $L/(n-1)$, as shown in Fig. 2(e).

The network model in Fig. 2(e) is the complete reconstruction of the circuit model between Sensor 1 and Sensor 2. We can similarly reconstruct the circuit model between Sensor 2 and Sensor 3, and also the circuit model between Sensor 3 and Senor 4. This will provide us with the circuit model for the entire network. Importantly, obtaining such model does *not* require any prior information about the network parameters.

IV. Event Location Identification

Consider the reconstructed feeder model in Fig. 2(e). It consists of n buses and $n-1$ lines. As shown in [8], if a waveform measurement unit (WMU) is installed at the beginning of the

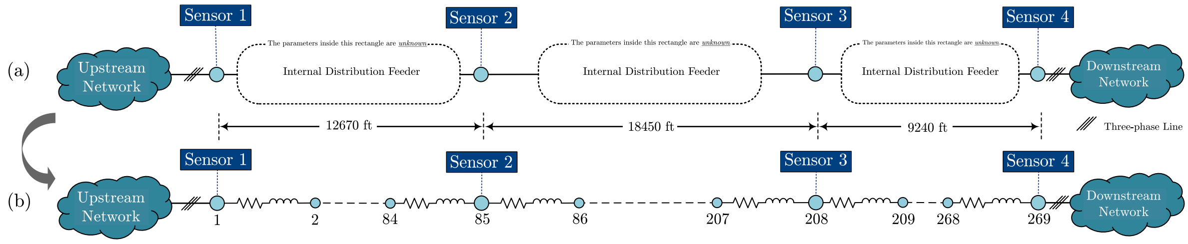

Fig. 3. The single line diagram of the real-world power distribution feeder in the United States, with four sites of sensors: (a) a picture of the distribution feeder, where no information about the structure and parameters between every two sensors is available; (b) the corresponding constructed feeder model with 269 buses.

feeder and another WMU is installed at the end of the feeder, the synchronized voltage and current waveform measurements from the two WMUs can be used to accurately identify the event bus by conducting a forward sweep and a backward sweep. In the forward sweep, we start from Sensor 1 at bus 1 and calculate the nodal voltages all the way to bus n. In the backward sweep, we start from Sensor 2 at bus n and calculate the nodal voltages all the way to bus 1. Suppose the location of the event is bus k. Parameter k is unknown. We can break down the calculations of the forward and backward sweeps into the following correct and incorrect calculations [8]:

$$\{\underbrace{V_1^f,\cdots,V_{k-1}^f,V_k^f}_{\text{correct}},\underbrace{V_{k+1}^f,\cdots,V_n^f}_{\text{incorrect}}\} \tag{10}$$

$$\{\underbrace{V_1^b,\cdots,V_{k-1}^b}_{\text{incorrect}},\underbrace{V_k^b,V_{k+1}^b,\cdots,V_n^b}_{\text{correct}}\} \tag{11}$$

where V_i^f and V_i^b denote the voltages at bus i that are calculated from forward and backward sweeps, respectively.

In (10)-(11), even though we do *not* know which bus is the event bus, we *do* know that the forward and backward voltage calculations at event bus k are correct. Since the *discrepancy* between the forward calculation and backward calculation is the lowest at event bus k, the event location is identified as [8]:

$$k^\star = \arg\min_i |V_i^f - V_i^b| = \arg\min_i \Psi_i, \tag{12}$$

where Ψ_i is the discrepancy at bus i.

The above analysis can be easily extended to the case with multiple line-mounted sensors. For example, in our real-world case, if the event occurs somewhere unknown between Sensor 2 and Sensor 3, then there are two different sets of discrepancy indexes to examine. One set is obtained by using the waveform measurements from Sensor 1 and Sensor 3, denoted by $\Psi_i^{1,3}$. Another set is obtained by using the waveform measurements from Sensor 2 and Sensor 4, denoted by $\Psi_i^{2,4}$. A combined discrepancy index can be defined as $\Psi_i = \Psi_i^{1,3} + \Psi_i^{2,4}$.

It bears mentioning that, if the event occurs on a lateral, our method can still identify the bus at the beginning of the lateral as the event bus. To identify the true location of the event, it is necessary to use a sensor at the end of the lateral [7].

Lemma 1: With two sensors, suppose the tuning operators for Sensors 1 and 2 are the same and equal to β. The value of β has no impact on identifying the location of the event.

Proof: From (5), and since $\Delta v_1(t) = \beta\Delta e_1(t)$ and $\Delta v_2(t) = \beta\Delta e_2(t)$, we have $\Delta V = \beta\Delta E$. Similar to (8), we can obtain:

$$\hat{P} = \beta\big((\Delta I^T \Delta I)^{-1}\Delta I^T \Delta E\big) = \beta\hat{P}^e \tag{13}$$

Thus, the estimated line parameters using the voltage waveforms are proportional, with ratio β, to the estimated line parameters by using the e-field waveforms. Let Z_i and Z_i^e be the impedance of line segment i that are estimated by using the voltage waveform and by using the e-field waveform,

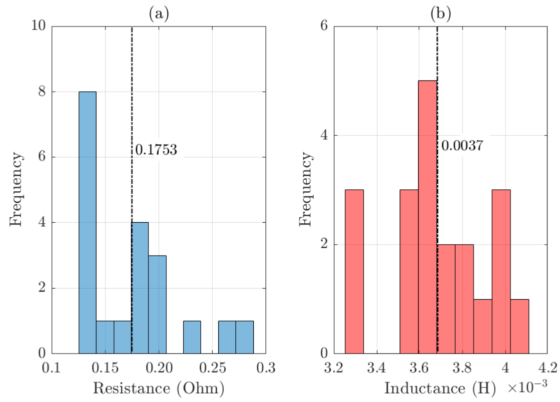

Fig. 4. Distribution of (a) the combined resistance; (b) the combined inductance of Phase B of the line between Sensors 1 and 2 using the proposed method in Section III. The means of the distributions are marked with dashed lines.

respectively, where $Z_i = \beta Z_i^e$. From the Kirchoff Voltage Law (KVL), we can obtain the nodal voltage in the forward sweep as $V_{i+1}^f = V_i^f - Z_i I_i^f$, see [7, Eq. (6)]. Thus, we have:

$$\beta E_{i+1}^f = \beta E_i^f - \beta Z_i^e I_i^f \quad \Rightarrow \quad E_{i+1}^f = E_i^f - Z_i^e I_i^f. \tag{14}$$

Parameter β is canceled out from the KVL equation. Similarly, we can derive an equation in the backward sweep as $E_{i+1}^b = E_i^b + Z_i^e I_i^b$, see [7, Eq. (11)]. Accordingly, we have: $|V_i^f - V_i^b| = \beta|E_i^f - E_i^b|$. Therefore, from (12), the value of tuning operator β has no impact in obtaining the location of the event. ∎

V. Real-World Case Study

The sensors in the real-world feeder in the United States are installed at four sites. We label each sensor separately at each phase, thus, we denote the sensors as: $1A, 1B, 1C, \ldots, 4A, 4B, 4C$. The synchronized waveform measurements are collected from all the sensors for 75 events that occurred over a period of six months, from March till August 2021.

A. Line Parameter Estimation Results

First, we use the synchronized waveform measurements during the 75 captured events to estimate the combined line parameters between every two adjacent sensors on the same phase. Fig. 4 shows the distribution of the combined resistance and the combined inductance of Phase B of the line between Sensor 1 and Sensor 2 using the method in Section III.

The distribution of the estimated inductance fluctuates over a narrow range, while the estimated resistance varies over a wider range. This is because most of the events in this study have resistive characteristics which affect the estimation of the combined resistance. The average resistance and the average inductance are marked on the dash lines. Table I shows the average value of the estimated line parameters of the lines between different sensors. For the rest of this paper, we use the average resistance and the average inductance of the lines.

TABLE I
RESULTS OF THE EVENT-BASED LINE PARAMETER ESTIMATION

Sensors	Phase A		Phase B		Phase C	
	R (Ohm)	L (H)	R (Ohm)	L (H)	R (Ohm)	L (H)
1 - 2	0.1888	0.0025	0.1753	0.0037	0.1775	0.0032
2 - 3	0.2443	0.0035	0.2237	0.0029	0.2021	0.0047
3 - 4	0.2005	0.0017	0.3238	0.0032	0.2047	0.0017

Once we estimated the line parameters, next we obtain the number of poles between every two adjacent sensors. The average distance between every two adjacent poles in this feeder is 150 ft. From (9), the number of poles/buses are obtained as: 85 poles between Sensors 1 and 2, 124 poles between Sensors 2 and 3, and 62 poles between Sensors 3 and 4. Thus, Sensor 1 is at bus 1, Sensor 2 is at bus 85, Sensor 3 is at bus $208 = 85+124-1$, and Sensor 4 is at bus $269 = 208+62-1$.

Fig. 3(b) shows the reconstructed model of the feeder. This model will be later used for event location identification.

B. Event Location Identification Results

Again consider the real-world waveform measurements in Fig. 1. Recall that the event in this figure occurred somewhere on Phase B between Sensor 2 and Sensor 3. Next, we apply the proposed event location identification method to identify the event bus based on the reconstructed model in Fig. 3(b).

Since we do *not* know which bus is the true event bus, we *cannot* verify the correctness of the event location identification results. However, we *can* check the *consistency* of the results across the following two independent sets of data: one set is the waveform data from Sensor $1B$ and Sensor $3B$ and the other set is the waveform data from Sensor $2B$ and Sensor $4B$.

First, consider the profile for the discrepancy index $\Psi_i^{1B,3B}$ for $i = 1, \ldots, 269$ in Fig. 5(a). The minimum is reached at bus 123. Next, consider the profile for the discrepancy index $\Psi_i^{2B,4B}$ for $i = 1, \ldots, 269$ in Fig. 5(b). The minimum is reached at bus 93. From the results in Figs. 5(a) and (b), the identified event buses are always between Sensor 2 and Sensor 3, which is correct. This confirms the accuracy of the proposed event location identification method.

Importantly, the results in Figs. 5(a) and (b) vary in a narrow rang of 31 buses from bus 93 to bus 123. Thus, it is expected that the exact location of the event, that we saw its waveforms in Fig. 1, is somewhere between bus 93 to bus 123. In this case, the identified zone of the event is at the downstream of Sensor 2 and somewhere between $150 \times (93 - 85 + 1) = 1350$ ft to $150 \times (123 - 85 + 1) = 5850$ ft. Accordingly, the identified event zone is $5850 - 1350 = 4500$ ft long.

The above results are much more specific than the initial event zone that we mentioned based on visual inspection in Section I. Note that, such initial event zone is somewhere between Sensor 2 and Sensor 3, which is 18450 ft; see Fig. 3. Thus, the proposed event location identification method is able to significantly narrow down the event zone by 76% from 18450 ft to 4500 ft. This confirms the effectiveness of the proposed method. We shall emphasize that this method does not use any prior knowledge about the network parameters.

Finally, if we sum up the above two discrepancy indexes, we can obtain a combined discrepancy index $\Psi_i = \Psi_i^{1B,3B} + \Psi_i^{2B,4B}$; see Fig. 5(c). The minimum of the combined discrepancy occurs at bus 105, which is inside the identified event zone from bus 93 to bus 123. This confirms the consistency of the proposed event location identification method.

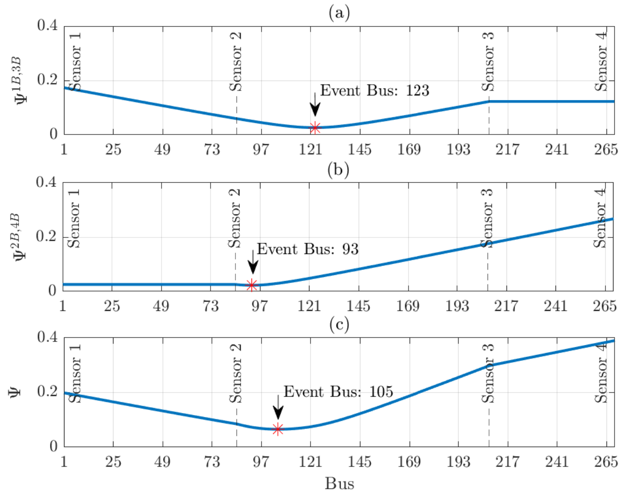

Fig. 5. Discrepancy index using the waveform measurements from: (a) Sensors $1B$ and $3B$; (b) Sensors $2B$ and $4B$; (c) Sensors $1B, 2B, 3B, 4B$.

VI. CONCLUSIONS

A model-free event location identification method was proposed to identify the location of events using real-world synchronzied e-field and current waveform data; *without* knowing the network parameters. The proposed method was applied to the real-world synchronized waveform measurements from 12 line-mounted sensors at four sites on a power distribution feeder in the United States. The results illustrated the accuracy, effectiveness, and consistency of the proposed method in identifying the correct location of events. On average, the proposed method is able to significantly narrow down the event zone by 76%.

REFERENCES

[1] [Online]. Available: https://www.sentient-energy.com
[2] S. Kulkarni, S. Santoso, and T. A. Short, "Incipient fault location algorithm for underground cables," *IEEE Trans. Smart Grid*, vol. 5, no. 3, pp. 1165–1174, May 2014.
[3] R. Krishnathevar and E. E. Ngu, "Generalized impedance-based fault location for distribution systems," *IEEE Trans. Power Deli.*, vol. 27, no. 1, pp. 449–451, Jan. 2012.
[4] H. Mohsenian-Rad, *Smart Grid Sensors: Principles and Applications*. Cambridge University Press, Cambridge, UK, 2022.
[5] L. Iurinic, A. Herrera-Orozco, R. Ferraz, and A. Bretas, "Distribution systems high-impedance fault location: A parameter estimation approach," *IEEE Trans. Power Deli.*, vol. 31, no. 4, pp. 1806–1814, Aug. 2016.
[6] A. Borghetti, M. Bosetti, C. A. Nucci, M. Paolone, and A. Abur, "Integrated use of time-frequency wavelet decompositions for fault location in distribution networks: theory and experimental validation," *IEEE Trans. Power Deli.*, vol. 25, no. 4, pp. 3139–3146, Oct. 2010.
[7] M. Izadi and H. Mohsenian-Rad, "Event location identification in distribution networks using waveform measurement units," in *Proc. IEEE PES ISGT Europe*, The Hague, Netherlands, 2020, pp. 924–928.
[8] M. Izadi and H. Mohsenian-Rad, "Synchronous waveform measurements to locate transient events and incipient faults in power distribution networks," *IEEE Trans. Smart Grid*, vol. 12, pp. 4295–4307, Sep. 2021.
[9] A. Bastos, S. Santoso, W. Freitas, and W. Xu, "Synchrowaveform measurement units and applications," in *Proc. IEEE PES General Meeting*, Atlanta, GA, USA, 2019, pp. 1–5.
[10] M. Izadi and H. Mohsenian-Rad, "Characterizing synchronized Lissajous curves to scrutinize power distribution synchro-waveform measurements," *IEEE Trans. Power Syst.*, pp. 1–4, May 2021.
[11] M. Izadi and H. Mohsenian-Rad, "A synchronized Lissajous-based approach to achieve situational awareness using synchronized waveform measurements," in *Proc. IEEE PES General Meeting*, Washington, DC, 2021, pp. 1–5.
[12] M. Izadi and H. Mohsenian-Rad, "A synchronized Lissajous-based method to detect and classify events in synchro-waveform measurements in power distribution networks," *IEEE Trans. Smart Grid*, Feb. 2022.
[13] K. Chen, X. Yang, and W. Xu, "Contactless voltage distortion measurement using electric field sensors," *IEEE Trans. Smart Grid*, vol. 9, no. 6, pp. 5643–5652, Nov. 2018.
[14] W. Zhang, C. Witharana, W. Li, C. Zhang, X. Li, and J. Parent, "Using deep learning to identify utility poles with crossarms and estimate their locations from google street view images," *Sensors*, vol. 18, Aug. 2018.